Analysis of carbon and nitrogen dynamics in riparian soils: Model validation and sensitivity to environmental controls

J. Batlle-Aguilar[1,4], A. Brovelli[1*], J. Luster[2], J. Shrestha[2], P.A. Niklaus[3], D.A. Barry[1]

[1] *Ecological Engineering Laboratory, Institute of Environmental Engineering, Faculté de l'Environnement Naturel, Architectural et Construit (ENAC), École Polytechnique Fédérale de Lausanne (EPFL), Station 2, 1015 Lausanne, Switzerland* (alessandro.brovelli@epfl.ch, andrew.barry@epfl.ch)

[2] *Soil Structure and Function Group, Swiss Federal Research Institute (WSL), 8903 Birmensdorf, Switzerland* (*joerg.luster@wsl.ch*, *juna.shrestha@wsl.ch*)

[3] *Institute of Evolutionary Biology and Environmental Studies, University of Zürich, 8057 Zürich, Switzerland* (*pascal.niklaus@ieu.uzh.ch*)

[4] *Now at National Centre for Groundwater Research and Training (NCGRT), School of the Environment, Flinders University, GPO Box 2100, Adelaide, South Australia 5001, Australia* (*jordi.batlleaguilar@flinders.edu.au*)

Accepted for publication in *Science of the Total Environment*

9 April 2012

* Corresponding author, ph.: +41 (0) 21 693 59 19, fax: +41 (0) 21 693 80 35

Abstract

The Riparian Soil Model (RSM) of Brovelli et al. (2012) was applied to study soil nutrient turnover in a revitalized section of the Thur River, North-East Switzerland. In the present work, the model was calibrated on field experimental data, and satisfactorily reproduced soil respiration, organic matter stocks and inorganic nitrogen fluxes. Calibrated rates were in good agreement with the ranges reported in the literature. The main discrepancies between model and observations were for dissolved organic carbon. The sensitivity of the model to environmental factors was also analysed. Soil temperature was the most influential factor at daily and seasonal scales while effects of soil moisture were weak overall. The ecosystem sensitivity to temperature changes was quantified using the Q10 index. The seasonal behaviour observed was related to the influence of other forcing factors and to the different state (density and activity) of the microbial biomass pool during the year. Environmental factors influencing microbial decomposition, such as the C:N ratio and litter input rate, showed intermediate sensitivity. Since these parameters are tightly linked to the vegetation type, the analysis highlighted the effect of the aboveground ecosystem on soil functioning.

Keywords: Ecological restoration; Riparian landscape; Nutrient cycles; Ecological Modelling; DOC mobilization; N removal

1 Introduction

Riparian zones are dynamic boundaries between terrestrial and aquatic systems, and play a paramount role in maintaining the vitality of landscapes and of surface water bodies (Naiman et al., 2000; Naiman and Décamps, 1997). These zones have key ecological functions: They act as ecological corridors and help preserve biodiversity in urban and industrialized environments (Goodwin et al., 1997; Martin and Chambers, 2002). Moreover, they have the ability to filter and clean-up polluted waters, preserving natural and healthy ecosystems. However, riparian zones are varied and not all function for instance as filters for polluted waters with the same effectiveness. For example, nitrate attenuation in riparian woodlands is significantly more effective than riparian grasslands (Lyons et al., 2000; Mayer et al., 2005), although their effectiveness was found to be lower in phosphate and dissolved organic phosphorous removal (Osborne and Kovacic, 1993). Nitrate is stored in biota via plant root uptake and microbial immobilization or converted to gaseous N_2 and nitrous oxide (N_2O) and removed via microbial denitrification (Klocker et al., 2009; Mander et al., 2005; Prober et al., 2005; Torok et al., 2000). Forest vegetation generally provides more organic matter in deeper subsoils than grassed lands, which is needed for effective denitrification in groundwater (Correll, 1997). Degradation of riparian woods engenders a loss of potential nitrate removal effectiveness.

Despite their importance, in the last century riparian areas were often profoundly modified and degraded, with a significant loss of ecological significance and functioning (Richardson et al., 2007). The trend has changed in recent years, with the design and implementation of a number of restoration projects, with the aim to re-establish the original natural status and conditions (Young et al., 2005). As a part of restoration design and for the assessment of the improved ecological status, numerical tools have been increasingly used to understand and forecast the modifications induced in ecosystems because of changes in land use, climatic parameters and management practices. Predictive models of soil organic matter (SOM) evolution include soil carbon (C) and N fluxes and their coupled dynamics. Numerous SOM models exist (Manzoni and Porporato, 2009), although only a few of them have been specifically developed, or adapted, to evaluate changes in ecosystem functioning in riparian areas (e.g.: SWIM, Hattermann et al., 2004; TNT2, Oehler et al., 2009).

Dissolved organic matter (DOM), which includes dissolved organic C (DOC) and N (DON), is an important controlling factor for the ecological functioning of forest soils (Michalzik et al., 2003) and grasslands (Kindler et al., 2011), as well as a major C source to mineral soils. For these reasons, their fate and dynamics are crucial for the prediction of organic C pools (Neff and Asner, 2001), in particular in riparian strips, which are influenced by the adjacent river and can have large external DOM inputs. The latter can occur, for example, during flood events, when unstructured soil material with labile organic matter is deposited (Samaritani et al., 2011). Despite their importance, DOM dynamics are frequently not accounted for when modelling soil nutrient turnover.

Within the soil, organic C is transferred between different pools by means of decomposition processes mediated by pedofauna. The activity of micro-organisms is regulated by environmental conditions, mainly soil moisture and temperature (Brady and Weil, 2004). The soil surface temperature signal is quickly dampened with depth and, at a depth of about 1 m, temperature variations are negligible compared with soil moisture changes (Rodriguez-Iturbe and Porporato, 2004). This argument has been used to explain partially the higher influence of soil moisture on microbial activity, in particular in dry environments (Bell et al., 2008; Davidson et al., 1998; Koch et al., 2007; Rodriguez-Iturbe and Porporato, 2004). Temperature changes at the daily and seasonal scales can result in topsoil temperature variations up to 5-10°C. Since the upper part of the soil profile is where OM is more abundant, in this shallow zone temperature is likely to have a large influence on microbial activity and C fluxes. The relationship between soil respiration (i.e., CO_2 emissions from a soil profile) and temperature has been investigated thoroughly. In this context, the parameter Q10, which indicates the increase in soil respiration for a 10°C increase in soil temperature, has been used to compare the sensitivity of different ecosystems (Beier et al., 2008). In well-drained, water-rich ecosystems, where moisture availability is seldom or never a limiting factor, temperature becomes the dominant forcing factor (Curiel Yuste et al., 2007).

In this paper, the Riparian Soil Model (RSM, Brovelli et al., 2012) was tested through application to a recently restored riparian ecosystem. The model was further applied to study the relationships between intertwined environmental parameters governing nutrient cycles in riparian systems at a daily time-scale. The field site, sampling and monitoring procedures are described in Sec. 2. Modelling results, validated with experimental measured data, are presented in Sec. 3. Finally, in Sec. 4 the model is used to study the effect of environmental controls in riparian soils.

2 Materials and methods

2.1 Field site

The research site was a revitalized section of the Thur River, near Niederneunforn, northeast Switzerland, with a mean altitude of about 375 m (Fig. 1). The Thur River is the largest Swiss river without a natural or artificial reservoir along its course, with a total length of 127 km and a catchment area of 1750 km^2. The river flows through an area of intensive agriculture and substantial urbanisation, and is heavily impacted by anthropogenic activities. At the experimental site, the riverbed crosses glacio-fluvial sandy gravel sediments of about 6-m thickness, which overlay impervious lacustrine clays (Vogt et al., 2010).

During restoration in 2002, the width of a section of the main river channel was doubled to about 100 m for 2.5 km by removal of overbank material and levees. Groundwater flows from the river towards the side channel, located at a distance of about 180 m in the alluvial forest. Over a distance of 40 to 60 m there is a lateral successional gradient from the river to the forest including bare gravel, gravel overlaid by fresh fluvial sediments, i.e., deposited after the restoration, colonized by mainly canary reed grass (*Phalaris arundinacea*), old overbank sediments planted with young willows (*Salix viminalis*) during the restoration, and finally the mature riparian hardwood forest developed on older overbank sediments with ash (*Fraximus excelsior* L.) and maple (*Ace* sp.) as the dominant trees. A footpath separates the willow bush zone and the forest.

The selected monitoring-sampling point F2 is located in the forest about 10 m from the footpath (Fig. 1). In spring, the ground vegetation is dominated by wild garlic (*Allium ursinum* L.), later in summer, *Aegopodium podagraria* L., *Rubus fructicosus* and nettle (*Urtica dioica* L.) become dominant. The alluvial soil is a carbonate-containing loam to silty-loam displaying little variation with depth (Table 1).

2.2 Soil sampling, processing and analysis

Samples for basic soil characterization were collected in May 2008. Within each of the three plots in the forest (with a diameter of 8 m), two cores were taken using a hand auger to a depth of 1 m and divided into 20 cm segments. For each plot, corresponding segments of the two cores were pooled for sample preparation and analysis. Samples were dried at 40°C and sieved to 2 mm. The clay (< 2 µm) and silt (2 – 63 µm) fractions were determined after removal of organic matter by treatment with hydrogen peroxide using the pipette method of Gee and Bauder (1986). Organic C contents of ground samples were determined with an elemental analyser (NC2500, CE Instruments, Italy) after removal of carbonates by acid treatment, and total N contents were determined on untreated samples using the same analyser (Walthert et al., 2010).

Between autumn 2008 and spring 2010, the water content at depths of 10 and 50 cm was measured at 30-min intervals at three replicate locations (parallel to river, 5.5 m distance between locations, 2 locations within sampling plot, 1 location outside) using EC-5 and EC-TM sensors (Decagon Devices Inc.). Raw signals were converted to volumetric water content using customized calibrations. For one of the three replicates for each depth, temperature was measured using EC-TM sensors.

Between autumn 2008 and autumn 2009, the soil efflux of CO_2 and N_2O was measured using a pre-installed PVC ring (30-cm diameter and 30-cm long inserted 20-cm deep in soil). Immediately before sampling, vegetation within the ring was clipped and the chamber closed with an airtight lid. Headspace air samples were collected after 5, 25 and 45 min, injected into pre-evacuated glass vials ('exetainers'), and analysed for CO_2 and N_2O concentrations using a gas chromatograph with an electron-capture detector (Agilent 6890, Santa Clara, USA). The soil-atmosphere N_2O exchange rate was calculated by linear regression of concentration against time. From April to October 2009 the sampling interval was 14 d on average, but higher and lower sampling frequencies were adopted after major flood events in June and July 2009 and dry periods in August and September, respectively.

The soil solution was regularly sampled between spring 2009 and spring 2010, until October 2009 at the same dates as the gas efflux, then in monthly intervals. Soil solution was collected using tension lysimeters based on ceramic suction cups (Soil Moisture Inc.) that were pre-installed at the same depths as and in close vicinity to the water content sensors. At each sampling, a constant vacuum was applied at -60 kPa for up to 2 d. The soil solution samples, as well as deposition and river water samples taken at the same time, were immediately filtered (0.45 μm) and stored at 2°C. These samples were analysed for NH_4 (flow injection analysis based on alkalinisation and diffusion of NH_3 into an acid carrier followed by colorimetric detection of an indicator dye), NO_3 (direct colorimetry, Navone 1964) and non-purgeable organic C (elemental analyser, Skalar Formacs HT and TN).

Samaritani et al. (2011) presented a study relating variability of C pools and fluxes (CO_2) to soil properties, environmental conditions and flood disturbance in a revitalized section of the Thur River. They found that, overall, environmental conditions driven by seasonality and flooding affected soil C dynamics more than soil properties did. In comparison with the frequently flooded gravel bars, the riparian forest, data of which are used in the present study, was rather stable with comparatively small spatial heterogeneity due to only rare flooding events. It was also characterized by relatively high organic C contents and water retention capacity both of which could be related to the relatively fine soil texture.

2.3 Soil C and N modelling

The data collected during 2008-2010 were used to validate the model of Brovelli et al. (2012). Ideally, model parameters should be independently measured through ad hoc laboratory experiments. Although attractive, this approach has shown limited applicability because in laboratory experiments conditions are idealized, and the computed parameters normally over-estimate the field values. On the other hand, field experiments cannot be used to infer directly the model parameters, as they are influenced by changing environmental conditions (moisture content, temperature, nutrient availability, etc). The calibration was therefore performed with a trial-and-error approach, during which model parameters controlling the different processes were tuned to match the measurements, in particular OM degradation and mobilization rates (k_l, k_h and k_d), respiration coefficients (r_h and r_r, respectively), plant uptake factors and nitrification/denitrification rates (k_n and k_{denit}, respectively).

Four external processes were assumed to drive the dynamics of SOM decomposition and nutrient turnover: precipitation, temperature, vegetation uptake (evapotranspiration, EVT, and N uptake) and organic matter release (litter inputs and root exudates):

Precipitation

Daily rainfall measurements at the Thur site recorded in parallel to soil data monitoring were used as input in the model (Fig. 2a).

Temperature

The soil surface temperature (at $z = 0$) and the thermal diffusivity of the soil are required as input in the RSM model to simulate the temperature profile. Air temperature measured at a meteorological station nearby the sampling point was applied as a boundary condition at the soil surface. Soil parameters (porosity and soil field capacity) were taken from the root zone and assumed constant along the soil profile to compute soil thermal capacity. Soil thermal conductivity was calibrated using the measured values at two depths (z_1 = 40 cm and z_2 = 100 cm) (Fig. 2b).

Vegetation uptake

Vegetation influences directly the soil moisture through transpiration and the mineral N stocks via plant root uptake. Plant transpiration was modelled in combination with evaporation as described by Brovelli et al. (2012), with parameters suitable for a forest soil (Batlle-Aguilar et al., 2011). The parameters needed in the model are listed in Table 2 and include the level of incipient stress (s^*), hygroscopic and wilting points (s_h and s_w, respectively), soil field capacity (s_{fc}) and the effect of temperature on plant transpiration (fT_r). Note that in the EVT modelling approach used by the RSM simulator, canopy interception is directly removed from precipitation, rather than being considered in the computations of EVT (see Rodriguez-Iturbe et al., 1999 for details). Plant physiological processes, transpiration and nutrient uptake in particular, vary temporally. The annual cycle of vegetation was introduced using the plant activity coefficient, as defined in Eq. (21) in Brovelli et al. (2012). The activity coefficient applied at the Thur site is shown in Fig. 2c (red dashed line). Parameters were taken from the literature, considering a similar vegetation and climate (Gu et al., 2008). Plant activity closely follows the annual temperature cycle, and therefore the activity coefficient is a maximum in late spring/early summer and starts to decline during July. From October to the end of the winter season plants are quiescent. Root uptake follows the same temporal dynamics of plant activity, with the maximum uptake occurring in late spring to sustain the vigorous plant growth.

Litter input and root exudates

Vegetation contributes to SOM through litter addition and production of root exudates. The timing, amount and C:N ratio of the OM released are all important factors for nutrient dynamics. The C:N ratio of the added litter (CN_{add}) is controlled by the vegetation type and is smaller for fallen leaves than for hardwood. An average value of 15 was used, which is suitable for Swiss forests (Heim and Frey, 2004; Tietema et al., 1998). Root exudates were assumed to have a higher N content, as vegetation produces these organic molecules to foster microbial communities in the root zone, and a value of 13 was used (Kuzyakov, 2002; Rovira, 1969). OM release follows an annual cycle, although litter production and root exudates have different timing. Root exudates are produced when the plant is active and therefore their dynamics are similar to that of transpiration and N uptake. Litter release has two components: One is constant through the year (for example, fallen branches and leaves after a storm or a fire, etc.), while the other has a peak in autumn due to falling leaves as plants enter the quiescent state. The amount of OM litter released from the vegetation is presented in Fig. 2c. Measurements of litter inputs at the Thur site were not available, and therefore literature values for similar vegetation, latitude and climatic conditions were adopted (Bell, 1978; Finzi et al., 2001).

3 Results

3.1 Environmental controls and moisture dynamics

The computed EVT (evaporation from the soil and plant transpiration) is shown in Fig. 2a. EVT is largest in early summer, when both plant transpiration and soil evaporation are near their maximum value (as temperature is also near its peak). EVT reaches its lowest value in winter, particularly January to February. Some of the parameters (particularly the maximum EVT rate and the minimum evaporation rate) were adjusted slightly to match the soil moisture data. However, it was found that, below a certain value, the minimum evaporation rate (0.5 mm m^{-2} d^{-1}) plays virtually no role, and therefore the estimated value might not be reliable. Although EVT data were not available to validate the simulation results, the model predicts that the total soil transpiration and evaporation is about 350 mm y^{-1}. The total evapotranspiration (i.e., including vegetation interception and evaporation) can be computed from the difference between infiltration and leakage, and amounts to about 710 mm y^{-1}, which compares well with other estimates and measurements for wet areas/shrubs/mixed forests at a similar latitude and altitude in the Thur catchment (Gurtz et al., 1999). Fig. 2b reports daily averages of soil temperature measurements (solid lines) and corresponding model predictions (dashed lines), at two different depths. These measurements were used only to calibrate the parameters for the temperature model. The comparison is satisfactory, and the thermal diffusivity (Table 3) falls within literature ranges for this soil type (Wu and Nofziger, 1999). The main noticeable difference for the measurements at z_1 (40-cm depth) is the presence of high frequency fluctuations (with a period of a few days and amplitude of about 3-5ºC) starting around the beginning of April 2009. These fluctuations were attributed to problems with the temperature sensors that were perhaps exposed directly to air due to the opening of cracks or earthworm channels during the summer period.

Field measurements and modelling results of water saturation in the topsoil (first 10 cm depth) and root zone (between 10 and 60 cm depth) are presented in Fig. 3, while the calibrated soil properties are listed in Table 2. Despite the simplicity of the moisture balance model, the simulations mimic well the temporal dynamics of water saturation in both soil layers. The comparison is, however, slightly better for the topsoil because the water dynamics in this layer are mainly controlled by precipitation/EVT and are less sensitive to soil properties. Due to heavy precipitation in the upper part of the catchment, the Thur River water level rose in mid-July 2009, but the nearby alluvial plain was not flooded. The groundwater level at a piezometer a few metres from the soil sampling point (R017) followed the river dynamics. The water table was only 0.4 m below the ground surface, while in normal conditions it is about 2-m deep (data not shown). This event was well reproduced by the model, resulting in nearly saturated conditions in the root zone and high saturation in the top soil (Fig. 3).The main discrepancy between measurements and simulations occurs in the initial period between November and December 2008. In these two months, the model systematically underpredicts the measured moisture content in both layers. The simulated topsoil data show temporal dynamics that are similar to the measurements, although shifted by about 0.2 towards drier conditions. A similar difference (but less pronounced) is also visible one year later, in November 2009. Groundwater elevation data at R017 showed that the water table rose in the same period, remaining at about 1 m below the soil surface. In the same period, the soil surface was partially ponded for some days.

3.2 Immobile OM pools and soil respiration

Soil respiration data and model predictions are reported in Fig. 4a, together with the temporal evolution of the C stored in the immobile OM pools (Fig. 4b-d for litter, humus and biomass, respectively). The calibrated biogeochemical parameters are listed in Table 4. Only the parameters for the topsoil and root zone are reported, for which experimental data were available. The default parameters used for the rest of the profile (compartments 3 and 4, parent material and aquifer, respectively) are identical to those listed by Brovelli et al. (2012, Table 2).

Table 5 summarizes experimental and modelled total organic C (C_{org}) and C:N ratios in the topsoil and root zone at the monitoring-sampling point. The model reproduces satisfactorily the field observations. The simulated C:N ratios are similar to the measured values, indicating that the value used for the litter input is appropriate. The predicted organic C (C_{org}) in the soil was computed as the average (±1 standard deviation) of the simulation results for a period of 5 y (after the model was run to reach pseudo-steady state, in order to remove the influence of the initial condition). Measurements are instead the average (±1 standard deviation) of different soil samples all collected at the same time. The predicted values fall well within the observed ranges. The comparison further indicates that the field heterogeneity (given by the standard deviation of C_{org}) is larger than the expected range of fluctuation over 1 year. This might result from local micro-topography, which leads to areas where OM accumulates and others where it is depleted.

Soil respiration (measured as soil CO_2 efflux) was assumed to be the cumulative microbial respiration (decomposition of organic matter) in the two uppermost compartments. The model assumes that all the CO_2 produced within the soil profile immediately reaches the atmosphere, that is, the diffusion time is negligible compared to the model's 1-d time step. The importance of root (or autotrophic) respiration has been highlighted recently, and it has been suggested that it could contribute up to half the total soil CO_2 efflux (Fenn et al., 2010; Subke et al., 2011). The RSM model does not consider it explicitly (i.e., as a separate CO_2 source), rather the total respiration (i.e., of roots and biomass) is computed. This is a convenient approximation because (i) the knowledge of the different respiration processes occurring in the rhyzosphere is still incomplete, and (ii) ad hoc experiments to evaluate the relative contribution of root respiration to CO_2 efflux – a necessary input for a model – are seldom, if ever, conducted. The model could be extended once more insights into these processes become available. Soil respiration was calibrated adjusting the decomposition rates and respiration efficiencies. Microbial decomposition rates were set to 10^{-6} m^3 d^{-1} gC^{-1} for litter (k_l) and humus (k_h), which are consistent with the estimates of Paul and Clark (1996) and Hefting et al. (2005). Following Jenkinson and Coleman (2008), the C litter input rate due to biomass lysis (release of compounds from cells of dead microorganisms), k_d, was fixed at 7.5×10^{-3} d^{-1}. Isohumic and respiration coefficients, r_h and r_r respectively, were calibrated as 0.27 and 0.60, respectively, in agreement with values reported by Brady and Weil (2004) and Nesme et al. (2005). The model reproduces satisfactorily the seasonal pattern observed in the experimental data ($R^2 \approx 0.75$), with respiration increasing from a minimum in winter to a maximum in early summer (Fig. 4a). A detailed analysis of the environmental factors influencing this increase is presented below. Here, we mention only that during calibration it was observed that the most influential parameter was the temperature sensitivity coefficient.

Clearly, the dynamics of respiration is linked to that of the immobile C pools, and a visual comparison indicates that the strongest (negative) correlation is between litter and biomass pools in the topsoil. The C litter pool (Fig. 4b, dashed line) shows the largest seasonal fluctuations, with the stored C reaching a maximum and a minimum at the end of the winter and summer seasons, respectively. The position of the peaks is offset in time compared to respiration. The accumulation of litter in the topsoil during autumn and winter is due to the combination of two processes, i.e., fallen leaves and accumulation of dead pedofauna. The two processes have different timing, the former has a maximum in October (Fig. 2c), while biomass accumulation is largest in January, corresponding to the lowest temperatures. In this period, biomass activity is a minimum, and the lysis rate exceeds the growth rate, with a net reduction of the biomass pool (Fig. 4d). On the contrary, during summer, biomass activity is high, the growth rate exceeds the lysis rate and the living biomass pool increases. In parallel, litter is consumed through soil respiration and converted to humus (Fig. 4c) and CO_2. For this reason, the humus pool shows a maximum in the same period, although the amplitude of the fluctuations is much smaller than for the other immobile C pools.

3.3 Dissolved organic matter (DOC and DON)

DOM sources are the dissolution of organic matter and plant root exudates. Litter and humus mobilisation rates, k_{Cl} and k_{Ch}, were calibrated, respectively, to 10^{-6} d^{-1} and 5×10^{-7} d^{-1}, which are consistent with the values reported by Bengtson and Bengtsson (2007). Root exudation rates were calibrated to 0.1 and 0.03 g m^{-3} d^{-1} for the topsoil and root zone, respectively. It is difficult to compare the exudates production rates with literature values because most available estimates were derived from measurements in laboratory-controlled conditions (for example, hydroponic setups). Moreover, root exudates are strongly variable in time – their production rate is affected by environmental factors, such as humidity, temperature, nutrient availability and vegetation type (Kuzyakov, 2002; Rovira, 1969). Despite this limitation, the values used in the model appear realistic when compared with literature values for forests. For example, although for a different vegetation (loblolly pine forest), Phillips et al. (2009), assuming a constant production rate, estimated from in situ measurement during the growing season a total of 9.4 g m^{-2} y^{-1}, which compares well with the value predicted using the RSM (7.3 g m^{-2} y^{-1}). The rates used in the model decrease with depth because the rate of exudate production depends on the root density and activity (Rovira, 1969): Since generally root density decreases almost exponentially with depth, the exudate production rate is much higher in the topsoil than in the root zone.

The modelled temporal evolution of the dissolved pools is compared with measurements in Fig. 5. For DOC, the topsoil measurements are reproduced correctly by the model, as indicated by the high R^2. Low DOC concentrations, in comparison with the immobile OM, occur because soluble C (i) is consumed rapidly by microbial pedofauna (in particular, low-molecular weight root exudates) and (ii) drains away with water flow. For the root zone, the model shows a trend similar to the experimental data, with a peak followed by a slow decrease. The peak is achieved about a month early, with a too-fast DOC accumulation in spring and early summer. A better fit (in terms of correlation coefficient) could be achieved by reducing the rate of root exudate production, but in this case simulations would miss the peak observed in late August. A possible explanation for the discrepancies is the partitioning or adsorption of DOC on the immobile OM or mineral solid phase (for example, clays) and colloids (Pérez et al., 2011; Schijf and Zoll, 2011), a process that is not included in the model. Simulated DON concentrations are also reported (Fig. 5b), but experimental data were not available. The same patterns observed for DOC were also found for DON, as the model assumes that organic matter dissolution influences C and N in a similar way, the only difference being the relative amounts, which are controlled by the C:N ratio.

3.4 Inorganic N

Mineral N pools are controlled by the balance between mineralization and immobilization (Porporato et al., 2003). In environments where N is abundant, such as the Thur site, organic N is available in excess and mineralization dominates over immobilization. Mineral N (in particular, nitrates) is removed by plants, leaches to the aquifer and a fraction is lost to the atmosphere through denitrification. This latter is a microbial anaerobic process that involves the use of nitrate as electron acceptor and its transformation to gaseous inorganic N. The reaction is complete when nitrates are converted to N_2, a situation that seldom occurs. Instead of N_2, N_2O is produced and released to the atmosphere. Although N_2O is produced also during nitrification, its main source is denitrification, and little is known about the environmental parameters that control its production (Del Grosso et al., 2000), although it is of great interest environmentally as it is a potent greenhouse gas (Cuhel et al., 2010). The denitrification rate depends on soil chemical and physical conditions such as oxygen content, temperature and pH (Heinen, 2006). Denitrification removes nitrate from the pore-water, and therefore nitrate leakage to the aquifer is reduced. This is a key ecological function of riparian buffers, which are able to reduce N inputs coming, for example, from fertilizers. To describe this process, RSM uses a first-order denitrification rate (k_{denit}) scaled by an activity coefficient that accounts for the water saturation level (and ultimately for oxygen availability). The denitrification rate resulting from calibration is 7.5×10^{-3} d^{-1}, which falls into the range of Heinen (2006), while the nitrification rate (k_{nit}) for the topsoil and root zone were calibrated as 0.005 and 2.25 g N m^{-3} d^{-1}, respectively (Table 4). Comparison of these values with literature ranges is difficult as in most cases a first-order nitrification rate is used. A model compatible with the RSM was used by D'Odorico et al. (2003). Compared to their calibrated values, the nitrification rates at the Thur site are about an order of magnitude higher for the root zone and two orders of magnitude lower for the topsoil. This discrepancy can be attributed to the different environmental conditions, as the work of D'Odorico et al. (2003) considered a savannah ecosystem, where climatic parameters and vegetation are very different from those at the Thur site. Further experimental work is necessary to elucidate in detail the nitrification rates and controlling factors in riparian environments with high anthropogenic nitrate inputs.

The total plant nitrogen uptake is related to a threshold rate for both ammonium and nitrate species (DEM^+ and DEM^-, respectively), which defines the actual uptake rate. DEM^+ and DEM^- were calibrated as 0.06 (topsoil and root zone) and 0.01 and 0.015 g N m^{-3} d^{-1} (topsoil and root zone, respectively), an order of magnitude smaller than those reported by D'Odorico et al. (2003) for savannah soils (Table 2). In arid environments, such as savannah, plants are well adapted to uptake quickly available soil N, as this is only available as pulses after short precipitation events (D'Odorico et al., 2003). In riparian soils like the Thur site, N is available the entire year, in particular during the growing season, thus plant uptake rates are lower but continuous during the year. Despite the higher rate, in the savannah the total amount of mineral N removed by plants during a year is lower than in deciduous forests with temperate climate.

NO_3^- concentrations and N_2O efflux with time are presented in Fig. 6. The NO_3^- dynamics are captured well by the model in both topsoil and root zone. The model is also able to reproduce the N_2O pulses, although timing and magnitude do not match. These pulses were due to two major flooding events, which caused wet conditions that favoured denitrification and N_2O emissions.

The mismatch in N_2O fluxes was not unexpected, because N_2O production is extremely variable as it depends on the local physical environment, physiological characteristics of the microbial community, C availability, redox potential and soil acidity (Firestone et al., 1980). Moreover, it should be considered that the model predicts the total inorganic N efflux (i.e., N_2 gas and N_2O), and the relative composition of the N flux varies with time. For this reason, it is expected that model results will over-predict the measured N_2O flux. Regarding the slightly different timing of the pulse, similar to soil respiration the model computes N efflux as sum of denitrification products in the topsoil and root zone, neglecting the diffusion/advection time through the soil profile. Moreover, the model assumes that the onset of wet conditions triggers immediately the denitrification reaction. This is not entirely correct, as nitrate reduction commences only when dissolved oxygen is consumed, a process that can introduce a lag time for denitrification (perhaps 1-2 d).

4 Sensitivity to environmental forcing

Numerous studies have highlighted that, at most temperate-climate sites, nutrient turnover is sensitive to both soil moisture and temperature (Curiel Yuste et al., 2007; Hagedorn et al., 2010; Pietikåinen et al., 2005). In arid and semi-arid environments with high constant temperatures, such as in the savannah (D'Odorico et al., 2003; Porporato et al., 2003; Rodriguez-Iturbe and Porporato, 2004), soil moisture is the main driver of OM cycling. The sensitivity of the different processes to each of these factors is still debated, and probably depends on the specific characteristics (geology, climate, etc.) of the site considered. Understanding the effect and relative sensitivity to changes in environmental variables is important in order to forecast future evolution of ecosystems when the environmental forcing factors change, for example restoration or climate change.

The sensitivity of C and N turnover to different environmental parameters in the forest near the restored Thur transect is presented in Figs. 7-9. Fig. 7a-b presents the influence of water saturation and temperature on soil respiration (CO_2 efflux), which is a good indicator of the soil microbial activity. Soil temperature and respiration show a positive correlation whereas the influence of water saturation is limited. This agrees with the observations of Bengtson and Bengtsson (2007) and Hui and Luo (2004) in forests with a similar climate, who reported that soil temperature is perhaps the most influential factor regulating CO_2 efflux. Davidson et al. (1998) studied the interplay between soil moisture and temperature in a hardwood forest in a temperate climate (i.e., in conditions comparable to those of the field site studied here), and observed that moisture becomes a critical parameter for nutrient turnover in dry periods with high temperature. At the Thur site, water availability is fairly constant across the year, and seldom falls below field capacity (Fig. 2).

To analyse the effect of temperature on the soil ecosystem, Q10 was computed using experimental data and model results for the period 2008-2009. A significantly different value was found for each period of the year: 2.9 for the period January-April, 2.1 for May-July and 1.3 for August-October. These values reproduce the seasonal variability observed by Xu and Qi (2001), with the annual minimum occurring in mid-late summer, and the maximum occurring in winter. The variability is associated with annual changes in soil functioning: In January, plants and microbial pedofauna are quiescent, and the increase in temperature occurring in March-April boosts their activity. In the following period (May-June), the turnover rate further accelerates, and reaches a plateau around mid-June (the relationship between microbial rates and temperature changes is highly non-linear, see Brovelli et al. (2012). Afterwards, the temperature decreases again, but the rates remain relatively high because, at the end of summer, living microbial biomass and litter are both abundant. The seasonal Q10 variability suggests that the effects of environmental factors on nutrient turnover and CO_2 fluxes must be considered on the seasonal scale, and that average annual values may not be indicative of the sensitivity of soil respiration to temperature changes. This is consistent with the findings of others (Gu et al., 2004, 2008 and references therein), who observed that the relationship between CO_2 efflux and soil temperature must always be corrected for the effect of other environmental parameters, in particular soil moisture.

Fig. 7c presents the relationship between NO_3 concentration and C:N ratio. Although the C:N ratio variations are small, a negative correlation is apparent. When the organic matter is N-poor (high C:N ratio), low NO_3 concentrations are observed, and vice-versa. Goodale and Aber (2001) and Ollinger et al. (2002) observed that high C:N ratios produced a strong N demand by heterotrophic soil microbes, leaving less N available for nitrification and subsequent nitrate leaching. This mechanism is compatible with measurements and predictions at the Thur site. N_2O emissions are controlled primarily by the moisture content (Brovelli et al., 2012), with pulses occurring in wet conditions (model results not shown). The effect of temperature on denitrification is instead almost negligible, as illustrated in Fig. 7d.

Similar to soil respiration, soil temperature and water saturation have a completely different influence on DOC. According to modelling results, soil temperature and DOC show a positive relationship, with high concentrations of organic C at high temperatures (Fig. 8a shows the results for the root zone). From the comparison, the discrepancies between model predictions and experimental data are clearly visible. In particular, the model consistently over-estimates the measurements at high temperature (> 16°C), whereas the measurements at low temperature are well reproduced. This indicates that the seasonal contribution of plant root exudates is over-estimated by the model or that the biomass uptake when soil temperature is optimal is too small. The relationship between soil temperature and DOC is however weaker than that with soil respiration, consistent with the results of Hagedorn et al. (2010). In contrast, water saturation has negligible influence on DOC, as highlighted in Fig. 8b. Experimental results confirmed the model results, therefore suggesting that the reason for the mismatch is not related to moisture dynamics.

The existence of a correlation between soil respiration and DOC concentration has been debated and no clear answer has been reached. Neff and Asner (2001) and Van Hees (2005) hypothesized that DOC was the main source of soil respiration. On the contrary, Bengtson and Bengtsson (2007) and Gödde et al. (1996) found that the CO_2 evolution and DOC concentration were not significantly correlated to each other as they are controlled by different processes and chemistry. The positive relationship between soil temperature, soil respiration and DOC was highlighted above. Simulation results show that the two variables are positively correlated (Fig. 9). The experimental data do not confirm the existence of a correlation, although they fall well within the range predicted by the model. On the other hand, analysis of the CO_2 sources based on model predictions indicates that, at the end of the growing season, consumption of root exudates can represent a significant CO_2 source, thus partially confirming the findings of Neff and Asner (2001) and Van Hees (2005). However, given the limited ability of the model to reproduce DOC in the root zone this conclusion should be further tested using additional experimental data.

5 Summary and conclusions

The Riparian Soil Model (RSM, Brovelli et al., 2012) was validated through application to a recently restored riparian ecosystem in North-East Switzerland. The model was further used to study the relationships between intertwined environmental parameters governing nutrient cycles in riparian systems.

Modelling results reflect parameter values, and accurate estimation of these values reduces model uncertainty. Experimental data often exhibit spatial and temporal variability due to heterogeneity, instrumental accuracy, amongst other factors occurring in the field. Nevertheless, model parameters were satisfactorily constrained by closely fitting the experimental field data. The model was able to reproduce well the experimental data for the immobile SOM pools, and for the inorganic N fluxes. In particular, the trends observed in the field were in most cases reproduced correctly, thus providing some confidence in the reliability of the model. Simulations less satisfactorily reproduced DOC data, in particular for the root zone. Numerical experiments were conducted to ascertain which process could be responsible for the mismatch, but no clear answer was found.

Soil temperature, with large daily and seasonal oscillations, was identified as the main environmental factor controlling the microbial processes. The effect of moisture content was limited, mainly because at the Thur River site moisture is never a limiting factor for the plants and soil biota.

At the Thur River site, N is abundant and does not limit OM turnover. During the warm period (April-September), organic N is available in excess and is converted to nitrate. Nitrate release is however particularly marked in July and August, since during spring vigorous vegetation growth takes up mineral N and reduces its concentration in the pore water. N availability is mainly controlled by the C:N ratio of the OM released by vegetation (plant litter and root exudates), which implies that the N cycle is regulated, at least in part, by vegetation composition.

The ecosystem sensitivity to soil temperature changes was quantified through the Q10 index and compared with previous results obtained in similar conditions. Results were in good agreement with literature values and, more importantly, the seasonal Q10 variability reported elsewhere was reproduced. This further confirms that analysis and predictions of soil CO_2 releases are only meaningful if conducted at the seasonal scale, including the effects of other relevant environmental forcing factors and the evolution and state of the soil biota.

Acknowledgements

This research is part of the RECORD project of the Competence Centre Environment and Sustainability (CCES, http://www.cces.ethz.ch/projects/nature/Record). Funding was provided by the Swiss National Science Foundation (grant 200021-113296). We thank Bertrand Fournier (University of Neuchâtel, Switzerland) for information on dominant plants, and Paolo Perona (EPFL, Switzerland) and Nicola Pasquale (ETHZ, Switzerland) for meteorological data.

References

Batlle-Aguilar J, Brovelli A, Porporato A, Barry DA. Modelling soil carbon and nitrogen cycles during land use change. A review. Agron. Sustain. Dev. 2011; 31: 251-274.

Brovelli A, Batlle-Aguilar J., Barry DA. Analysis of carbon and nitrogen dynamics in riparian soils. Model development. Submitted to Sci. Total Environ. 2012.

Beier C, Emmett BA, Peñuelas J, Schmidt IK, Tietema A, Estiarte M, et al. Carbon and nitrogen cycles in European ecosystems respond differently to global warming. Sci. Total Environ. 2008; 407: 692-697.

Bell C, McIntyre N, Cox S, Tissue D, Zak J. Soil microbial responses to temporal variations of moisture and temperature in a Chihuahuan desert grassland. Microb. Ecol. 2008; 56: 153-167.

Bell DT. Dynamics of litter fall, decomposition, and incorporation in the streamside forest ecosystem. Oikos 1978; 30: 76-82.

Bengtson P, Bengtsson G. Rapid turnover of DOC in temperate forests accounts for increased CO_2 production at elevated temperatures. Ecol. Lett. 2007; 10: 783-790.

Brady NC, Weil RR. Elements of the nature and properties of soils. New Jersey (USA): Pearson Prentice Hall, 2004.

Correll DL. Buffer zones and water quality protection: general principles. In: Haycock NE, Burt TP, Goulding KWT, Pinay G, editors. International Conference on Buffer Zones, 1997, pp. 7-20.

Cuhel J, Simek M, Laughlin RJ, Bru D, Cheneby D, Watson CJ, et al. Insights into the effect of soil pH on N_2O and N_2 emissions and denitrifier community size and activity. Appl. Environ. Microbiol. 2010; 76: 1870-1878.

Curiel Yuste J, Baldocchi DD, Gershenson A, Goldstein A, Misson L, Wong S. Microbial soil respiration and its dependency on carbon inputs, soil temperature and moisture. Global Change Biol. 2007; 13: 2018-2035.

D’Odorico P, Laio F, Porporato A, Rodriguez-Iturbe I. Hydrologic controls on soil carbon and nitrogen cycles. II. A case study. Adv. Water Resour. 2003; 26: 59-70.

Davidson EA, Belk E, Boone RD. Soil water content and temperature as independent or confounded factors controlling soil respiration in a temperate mixed hardwood forest. Global Change Biol. 1998; 4: 217-227.

Del Grosso SJ, Parton WJ, Mosier AR, Ojima DS, Kulmala AE, Phongpan S. General model for N_2O and N_2 gas emissions from soils due to denitrification. Global Biogeochem. Cy. 2000; 14: 1045-1060.

Fenn KM, Malhi Y, Morecroft MD. Soil CO_2 efflux in a temperate deciduous forest: Environmental drivers and component contributions. Soil Biol. Biochem. 2010; 42: 1685-1693.

Finzi AC, Allen AS, DeLucia EH, Ellsworth DS, Schlesinger WH. Forest litter production, chemistry, and decomposition following two years of free-air CO_2 enrichment. Ecology 2001; 82: 470-484.

Firestone MK, Firestone RB, Tiedje JM. Nitrous oxide from soil denitrification: Factors controlling its biological production. Science 1980; 208: 749-751.

Gee GW, Bauder JW. Particle-size analysis. In: Klute A, editor. Methods of soil analysis, part 1, Physical and mineralogical methods. ASA, Agronomy monographs 9(1), Madison, Wisconsin, USA, 1986, pp. 383-411.

Gödde M, David MB, Christ MJ, Kaupenjohann M, Vance GF. Carbon mobilization from the forest floor under red spruce in the northeastern U.S.A. Soil Biol. Biochem. 1996; 28: 1181-1189.

Goodale CL, Aber JD. The long-term effects of land-use history on nitrogen cycling in northern hardwood forests. Ecol. Appl. 2001; 11: 253-267.

Goodwin CN, Hawkins CP, Kershner JL. Riparian restoration in the western United States: Overview and perspective. Rest. Ecol. 1997; 5: 4-14.

Gu L, Hanson PJ, Mac Post W, Liu Q. A novel approach for identifying the true temperature sensitivity from soil respiration measurements. Global Biogeochem. Cy. 2008; 22. DOI: doi:10.1029/2007GB003164.

Gu L, Post WM, King AW. Fast labile carbon turnover obscures sensitivity of heterotrophic respiration from soil to temperature: A model analysis. Global Biogeochem. Cy. 2004; 18: GB1022 1-11. DOI: 10.1029/2003GB002119.

Gurtz J, Baltensweiler A, Lang H. Spatially distributed hydrotope-based modelling of evapotranspiration and runoff in mountainous basins. Hydrol. Proc. 1999; 13: 2751-2768.

Hagedorn F, Martin M, Rixen C, Rusch S, Bebi P, Zürcher A, et al. Short-term responses of ecosystem carbon fluxes to experimental soil warming at the Swiss alpine treeline. Biogeochemistry 2010; 97: 7-19.

Hattermann F, Krysanova V, Wechsung F, Wattenbach M. Integrating groundwater dynamics in regional hydrological modelling. Environ. Model. Softw. 2004; 19:1039-1051.

Hefting MM, Clement J-C, Bienkowski P, Dowrick D, Guenat C, Butturini A, et al. The role of vegetation and litter in the nitrogen dynamics of riparian buffer zones in Europe. Ecol. Eng. 2005; 24: 465-482.

Heim A, Frey B. Early stage litter decomposition rates for Swiss forests. Biogeochemistry 2004; 70: 299-313.

Heinen M. Simplified denitrification models: Overview and properties. Geoderma 2006; 133: 444-463.

Hui D, Luo Y. Evaluation of soil CO_2 production and transport in Duke Forest using a process-based modeling approach. Global Biogeochem. Cycles 2004; 18: GB4029.

Jenkinson DS, Coleman K. The turnover of organic carbon in subsoils. Part 2. Modelling carbon turnover. Eur. J. Soil Sci. 2008; 59: 400-413.

Kindler R, Siemens J, Kaiser K, Walmsley DC, Bernhofer C, Buchmann N, et al. Dissolved carbon leaching from soil is a crucial component of the net ecosystem carbon balance. Global Change Biol. 2011; 17: 1167-1185.

Klocker C, Kaushal S, Groffman P, Mayer P, Morgan R. Nitrogen uptake and denitrification in restored and unrestored streams in urban Maryland, USA. Aquat. Sci. 2009; 71: 411-424.

Koch O, Tscherko D, Kandeler E. Temperature sensitivity of microbial respiration, nitrogen mineralization, and potential soil enzyme activities in organic alpine soils. Global Biogeochem. Cy. 2007; 21: GB4017.

Kuzyakov Y. Review: Factors affecting rhizosphere priming effects. Journal of Plant Nutrition and Soil Science-Zeitschrift Fur Pflanzenernahrung Und Bodenkunde 2002; 165: 382-396.

Lyons J, Thimble SW, Paine LK. Grass versus trees: Maintaining riparian areas to benefit streams of central North America. J. Am. Water Resour. Assoc. 2000; 36: 919-930.

Mander Ü, Hayakawa Y, Kuusemets V. Purification processes, ecological functions, planning and design of riparian buffer zones in agricultural watersheds. Ecol. Eng. 2005; 24: 421-432.

Manzoni S, Porporato A. Soil carbon and nitrogen mineralization: Theory and models across scales. Soil Biol. Biochem. 2009; 41: 1355-1379.

Martin D, Chambers J. Restoration of riparian meadows degraded by livestock grazing: Above and belowground responses. Plant Ecol. 2002; 163: 77-91.

Mayer PM, Reynolds SK, Canfield TJ. Riparian buffer width, vegetative cover, and nitrogen removal effectiveness: A review of current science and regulations. US EPA, 2005, 99. 40.

Michalzik B, Tipping E, Mulder J, Lancho JFG, Matzner E, Bryant CL, et al. Modelling the production and transport of dissolved organic carbon in forest soils. Biogeochemistry 2003; 66: 241-264.

Naiman RJ, Bilby RE, Bisson PA. Riparian ecology and management in the pacific coastal rain forest. Bioscience 2000; 50: 996-1011.

Naiman RJ, Décamps H. The ecology of interfaces: Riparian zones. Ann. Rev. Ecol. Syst. 1997; 28: 621-658.

Neff JC, Asner GP. Dissolved organic carbon in terrestrial ecosystems: Synthesis and a model. Ecosystems 2001; 4: 29-48.

Nesme T, Bellon S, Lescourret F, Senoussi R, Habib R. Are agronomic models useful for studying farmers' fertilisation practices? Agr. Syst. 2005; 83: 297-314.

Oehler F, Durand P, Bordenave P, Saadi Z, Salmon-Monviola J. Modelling denitrification at the catchment scale. Sci. Total Environ. 2009; 1726-1737.

Ollinger SV, Smith ML, Martin ME, Hallett RA, Goodale CL, Aber JD. Regional variation in foliar chemistry and cycling among forests of diverse history and composition. Ecology 2002; 83: 339-355.

Osborne LL, Kovacic DA. Riparian vegetated buffer strips in water-quality restoration and stream management. Freshwater Biol. 1993; 29: 243-258.

Paul EA, Clark FE. Soil microbiology and biochemistry. San Diego (USA): Academic Press, 1996.

Pérez MAP, Moreira-Turcq P, Gallard H, Allard T, Benedetti MF. Dissolved organic matter dynamic in the Amazon basin: Sorption by mineral surfaces. Chem. Geol. 2011; 286: 158-168.

Phillips RP, Bernhardt ES, Schlesinger WH. Elevated CO_2 increases root exudation from loblolly pine (Pinus taeda) seedlings as an N-mediated response. Tree Physiol. 2009; 29: 1513-1523.

Pietikåinen J, Pettersson M, Bååth E. Comparison of temperature effects on soil respiration and bacterial and fungal growth rates. FEMS Microbiol. Ecol. 2005; 52: 49-58.

Porporato A, D'Odorico P, Laio F, Rodriguez-Iturbe I. Hydrologic controls on soil carbon and nitrogen cycles. I. Modelling scheme. Adv. Water Resour. 2003; 26: 45-58.

Prober SM, Thiele KR, Koen LTB. Restoring ecological function in temperate grassy woodlands: Manipulating soil nutrients, exotic annuals and native perennial grasses through carbon supplements and spring burns. J. Appl. Ecol. 2005; 42: 1073-1085.

Richardson DM, Holmes PM, Esler KJ, Galatowitsch SM, Stromberg JC, Kirkman SP, et al. Riparian vegetation: Degradation, alien plant invasions, and restoration prospects. Div. Distrib. 2007; 13: 126-139.

Rodriguez-Iturbe I, Porporato A. Ecohydrology of water-controlled ecosystems. Soil moisture and plant dynamics. Cambridge, United Kingdom: Cambridge University Press, 2004.

Rodriguez-Iturbe I, Porporato A, Ridolfi L, Isham V, Cox DR. Probabilistic modelling of water balance at a point: The role of climate, soil and vegetation. Proc. R. Soc. Lond. A 1999; 455: 3789-3805.

Rovira AD. Plant root exudates. The Botanical Review 1969; 35: 35-57.

Samaritani E, Shrestha J, Fournier B, Frossard E, Gillet F, Guenat C, et al. Heterogeneity of soil carbon pools and fluxes in a channelized and a restored floodplain section (Thur River, Switzerland). Hydrol. Earth Sys. Sci. Discuss. 2011; 8: 1059-1091.

Schijf J, Zoll AM. When dissolved is not truly dissolved - The importance of colloids in studies of metal sorption on organic matter. J. Colloid Interf. Sci. 2011; 361: 137-147.

Subke JA, Voke NR, Leronni V, Garnett MH, Ineson P. Dynamics and pathways of autotrophic and heterotrophic soil CO_2 efflux revealed by forest girdling. J. Ecol. 2011; 99: 186-193.

Tietema A, Boxman AW, Bredemeier M, Emmett BA, Moldan F, Gundersen P, et al. Nitrogen saturation experiments (NITREX) in coniferous forest ecosystems in Europe: A summary of results. Environ. Pollut. 1998; 102: 433-437.

Torok K, Szili-Kovacs T, Halassy M, Toth T, Hayek Z, Paschke MW, et al. Immobilization of soil nitrogen as a possible method for the restoration of sandy grassland. Appl. Veg. Sci. 2000; 3: 7-14.

van Hees PAW, Jones DL, Finlay R, Godbold DL, Lundström US. The carbon we do not see -- The impact of low molecular weight compounds on carbon dynamics and respiration in forest soils: A review. Soil Biol. Biochem. 2005; 37: 1-13.

Vogt T, Schneider P, Hahn-Woernle L, Cirpka OA. Estimation of seepage rates in a losing stream by means of fiber-optic high-resolution vertical temperature profiling. J. Hydrol. 2010; 380: 154-164.

Walthert L, Graf U, Kammer A, Luster J, Pezzotta D, Zimmermann S, et al. Determination of organic and inorganic carbon, $\delta^{13}C$ and nitrogen in soils containing carbonates after acid fumigation with HCl. J. Plant Nutr. Soil Sci. 2010; 173: 207-216.

Wu J, Nofziger DL. Incorporating temperature effects on pesticide degradation into a management model. J. Environ. Qual. 1999; 28: 92-100.

Xu M, Qi Y. Soil-surface CO_2 efflux and its spatial and temporal variations in a young ponderosa pine plantation in northern California. Glob. Change Biol. 2001: 7: 667-677.

Young TP, Petersen DA, Clary JJ. The ecology of restoration: historical links, emerging issues and unexplored realms. Ecol. Lett. 2005; 8: 662-673.

Figure captions

Figure 1. Restored Thur River site (Switzerland) and location of the monitoring point F2.

Figure 2. (a) Measured rainfall and computed total EVT (topsoil + root zone) for the modelled period, 2008-2010; (b) measured and modelled soil temperature in the topsoil and root zone; (c) computed plant activity coefficient and total litter input (topsoil + root zone).

Figure 3. Measured and modelled water saturation in the topsoil (a) and root zone (b).

Figure 4. Modelled temporal concentrations of immobile organic matter: (a) litter; (b) humus; (c) biomass; (d) Measured and computed soil respiration.

Figure 5. Measured and modelled concentration of dissolved organic C, DOC (a) and simulated dissolved organic N, DON (b), in the topsoil and root zone.

Figure 6. (a) Measured and modelled concentration of nitrate (NO_3^-) in the topsoil and root zone; (b) measured and modelled concentration of nitrous oxide (N_2O).

Figure 7. Influence of (a) water saturation (topsoil) and (b) soil temperature (1-m depth) over soil respiration (CO_2). (c) Influence of C:N ratio on nitrate (topsoil); and (d) influence of soil temperature (1-m depth) on nitrous oxide production.

Figure 8. Influence of (a) soil temperature; and (b) water saturation, on dissolved organic C at 40-cm depth.

Figure 9. Modelled and experimental relationships between DOC and soil respiration (CO_2) at 50-cm depth.

Tables

Table 1. Soil properties measured in the mixed riparian forest (mean values ± SDEV, 3 samples were considered).

Depth (m)	Clay (%)	Silt (%)	Sand (%)	C org. (g kg^{-1})
0 – 0.2	18.9 ± 1.9	55.6 ± 3.1	25.5 ± 4.9	15.2 ± 4.3
0.2 – 0.4	16.1 ± 1.3	48.9 ± 2.6	34.9 ±3.9	13.2 ± 1.6
0.4 – 0.6	16.7 ± 0.9	49.3 ± 2.8	33.9 ± 2.5	10.6 ± 2.3
0.6 – 0.8	18.2 ± 3.4	53.1 ± 4.8	28.7 ± 7.6	14.2 ± 7.6
0.8 – 1.0	19.2 ± 3.0	53.7 ± 6.7	27.1 ± 9.3	10.5 ± 2.2

Table 2. RSM validated soil and plant properties.

		Soil compartment (*i*)	
		Topsoil	**Root zone**
Incipient stress ($s*$)	-	0.16	0.15
Hygroscopic point (s_h)	-	0.02	0.02
Wilting point (s_w)	-	0.05	0.05
Soil porosity (n)	-	0.53	0.38
Soil thickness (Zr)	m	0.25	0.90
Soil tortuosity index (d)	-	1.50	1.50
Soil field capacity (s_{fc})	-	0.50	0.57
Aquifer recharge threshold value (q_{tv})	m d^{-1}	-	-
Plant nitrate demand (DEM^-)	gN m^{-3} d^{-1}	0.01	0.015
Plant ammonium demand (DEM^+)	gN m^{-3} d^{-1}	0.06	0.06
Evapotranspiration wilting point (E_w)	m d^{-1}	0.001	0.005
G	-	2.0×10^{-4}	2×10^{-5}
L	-	0.2	1.0
fTr		4.0×10^{-4}	1.5×10^{-4}
Maximum root exudates production rate (RE^{max})	g m^{-3} d^{-1}	0.1	0.03

Table 3. RSM validated soil temperature parameters.

Parameter	Units	Value
Effective thermal diffusivity (D_h)	$m^2\ d^{-1}$	1.65×10^{-2}
Optimal temperature	°C	25
Temperature sensitivity, decomposition (υ_D QUOTE)	°C	0.07
Temperature sensitivity, nitrification/denitrification (υ_D)	°C	0.13
Amplitude of the yearly temperature signal (A_1)	°C	13.21
Amplitude of the daily temperature signal (A_2)	°C	1.5

Table 4. RSM calibrated biogeochemical parameters.

		Soil compartment (i)	
		Topsoil	**Root zone**
C:N ratio of biomass pool (CN_b)	-	13.5	11.5
C:N ratio of root exudates (CN_r)	-	12	
C:N ratio of added litter (CN_{Add})	-	15	
Litter decomposition rate (k_l)	$m^3\ d^{-1}\ gC^{-1}$	5.0×10^{-6}	7.75×10^{-6}
Humus decomposition rate (k_h)	$m^3\ d^{-1}\ gC^{-1}$	3.25×10^{-6}	3.75×10^{-6}
Rate of C return to litter pool (k_d)	d^{-1}	7.5×10^{-3}	
Litter pool mobilisation rate (k_{Cl})	d^{-1}	1.0×10^{-6}	
Humus pool mobilisation rate (k_{Ch})	d^{-1}	0.5×10^{-6}	
Dissolved C rate returning to biomass pool (k_{DC})	$m^3\ gC^{-1}\ d^{-1}$	1.5×10^{-6}	
Fraction of soluble humus (m_h)	-	0.20	
Fraction of soluble litter (m_l)	-	0.40	
Isohumic coefficient (r_h)	-	0.27	
Respiration coefficient (r_r)	-	0.60	
Fraction of dissolved ammonium (*a_amm*)	**-**	**0.05**	
Fraction of dissolved nitrate (*a_nit*)	-	1.0	0.5
Ammonium immobilisation coefficient (k^+)	$m^3\ d^{-1}\ gN^{-1}$	0.1	
Nitrate immobilisation coefficient (k^-)	$m^3\ d^{-1}\ gN^{-1}$	0.1	
Nitrification rate (k_{nit})	$m^3\ d^{-1}\ gN^{-1}$	0.005	2.25
Denitrification rate (k_{denit})	d^{-1}	$7.5\ \_\ 10^{-3}$	

Table 5. Measured and computed C:N ratios and C_{org} concentrations for topsoil and root zone layers (values in brackets indicate standard deviation).

C:N ratios	**Measured**	**Modelled**
Topsoil	13.11 (± 2.36)	14.92 (± 0.004)
Root zone	14.02 (± 1.83)	13.95 (± 0.003)
C_{org} (g Kg soil $^{-1}$)	**Measured**	**Modelled**
Topsoil	15.22 (± 4.30)	9.74 (± 0.46)
Root zone	12.11 (± 3.42)	9.60 (± 0.03)

Figures

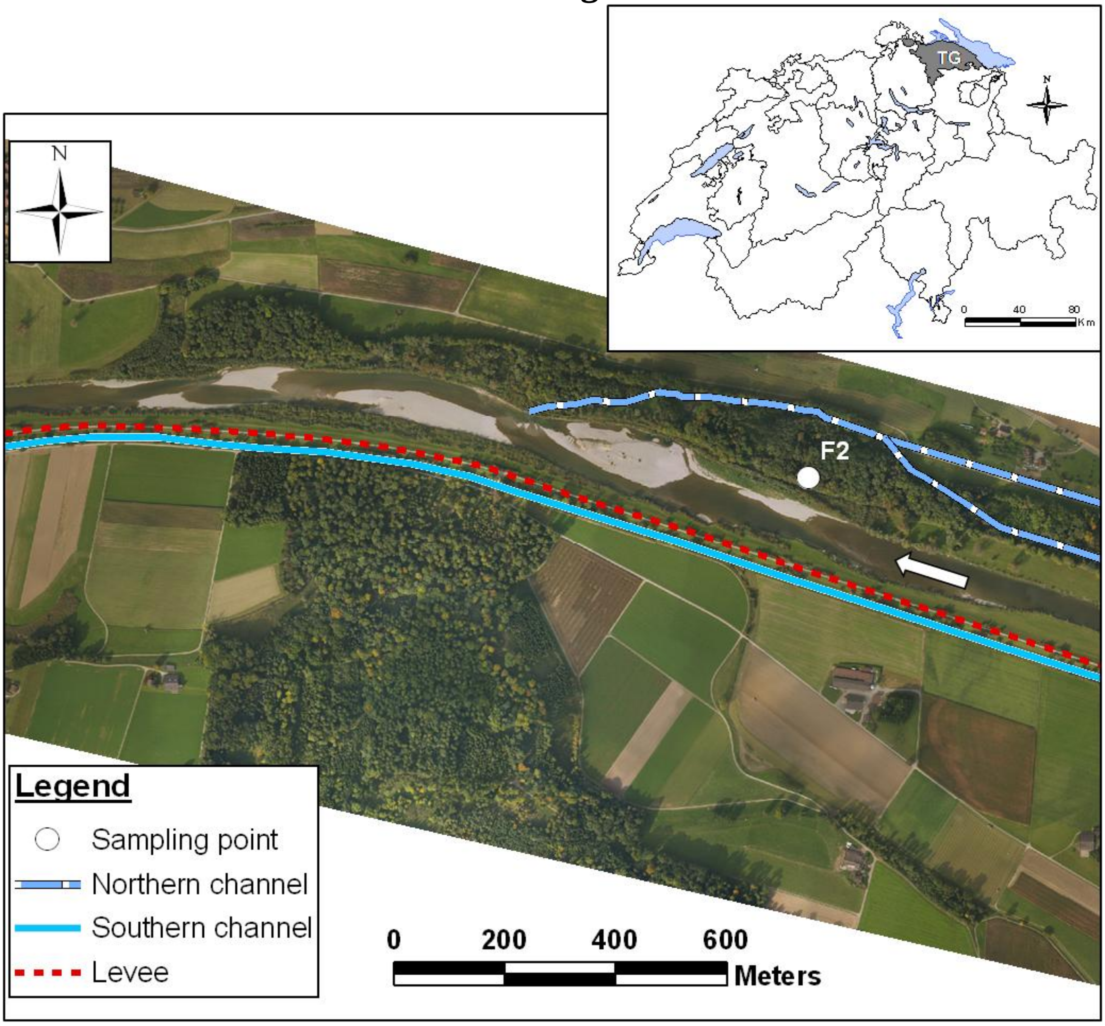

Fig. 1

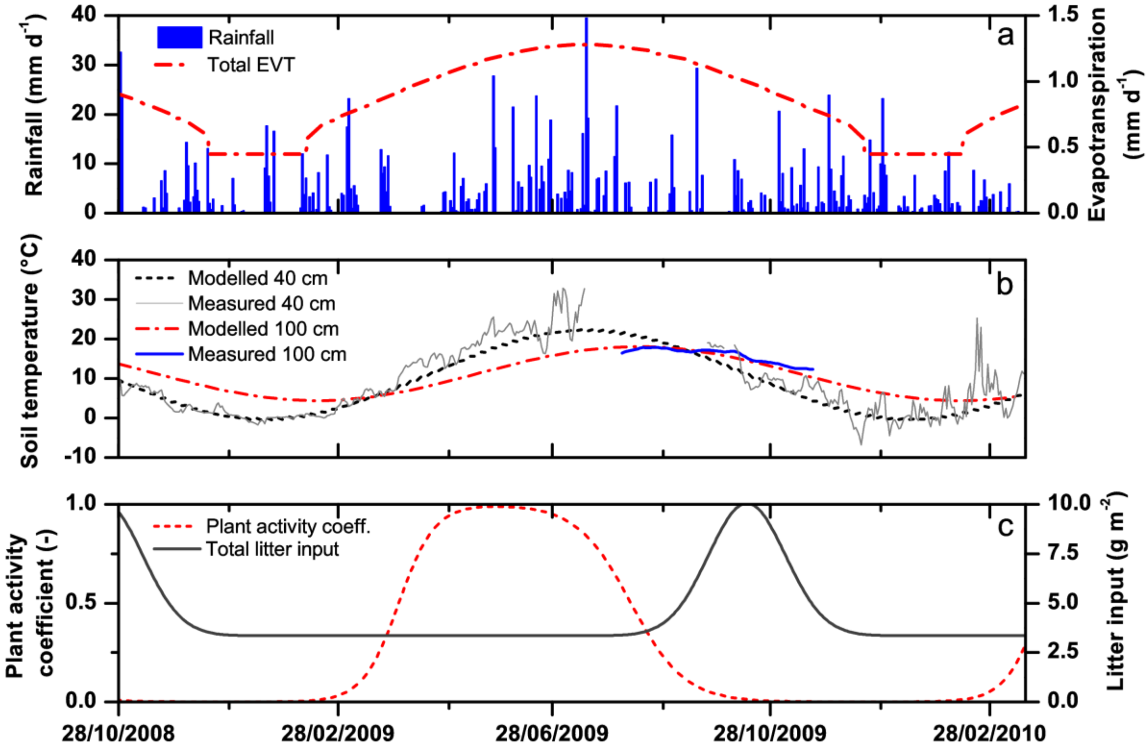
a
Rainfall
Total EVT
Rainfall (mm d-1)
Evapotranspiration (mm d-1)
b
Modelled 40 cm
Measured 40 cm
Modelled 100 cm
Measured 100 cm
Soil temperature (°C)
c
Plant activity coeff.
Total litter input
Plant activity coefficient (-)
Litter input (g m-2)
28/10/2008
28/02/2009
28/06/2009
28/10/2009
28/02/2010

Fig. 2

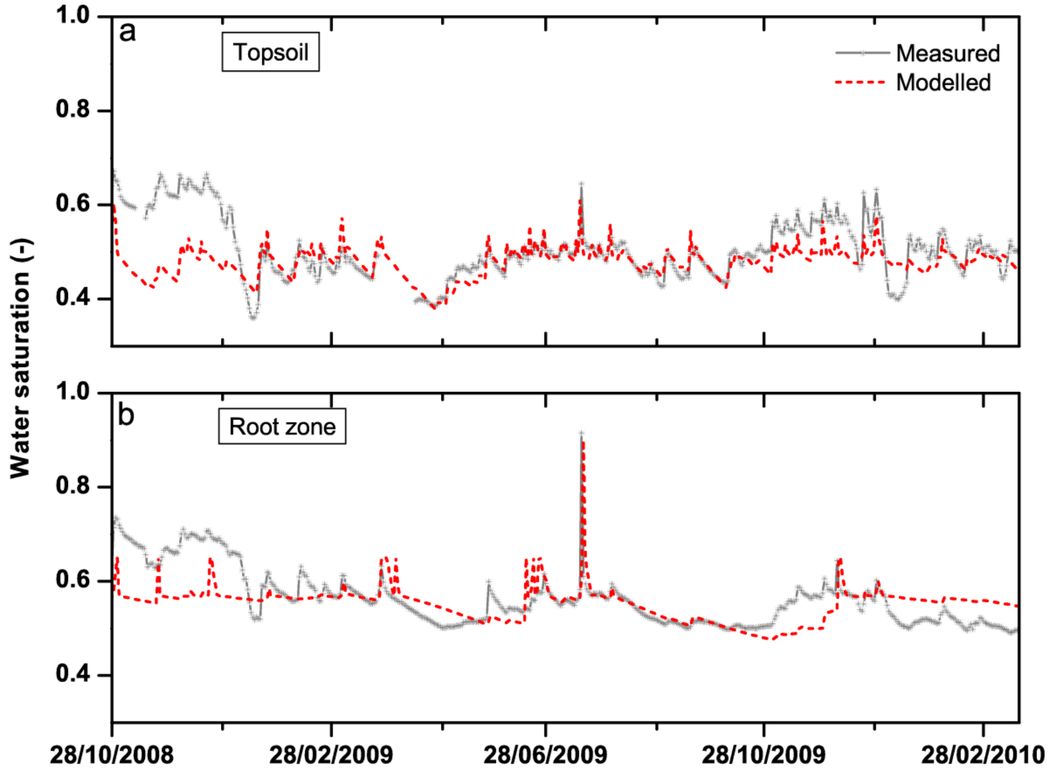
a
Topsoil
Measured
Modelled
b
Root zone
Water saturation (-)
1.0
0.8
0.6
0.4
28/10/2008
28/02/2009
28/06/2009
28/10/2009
28/02/2010

Fig. 3

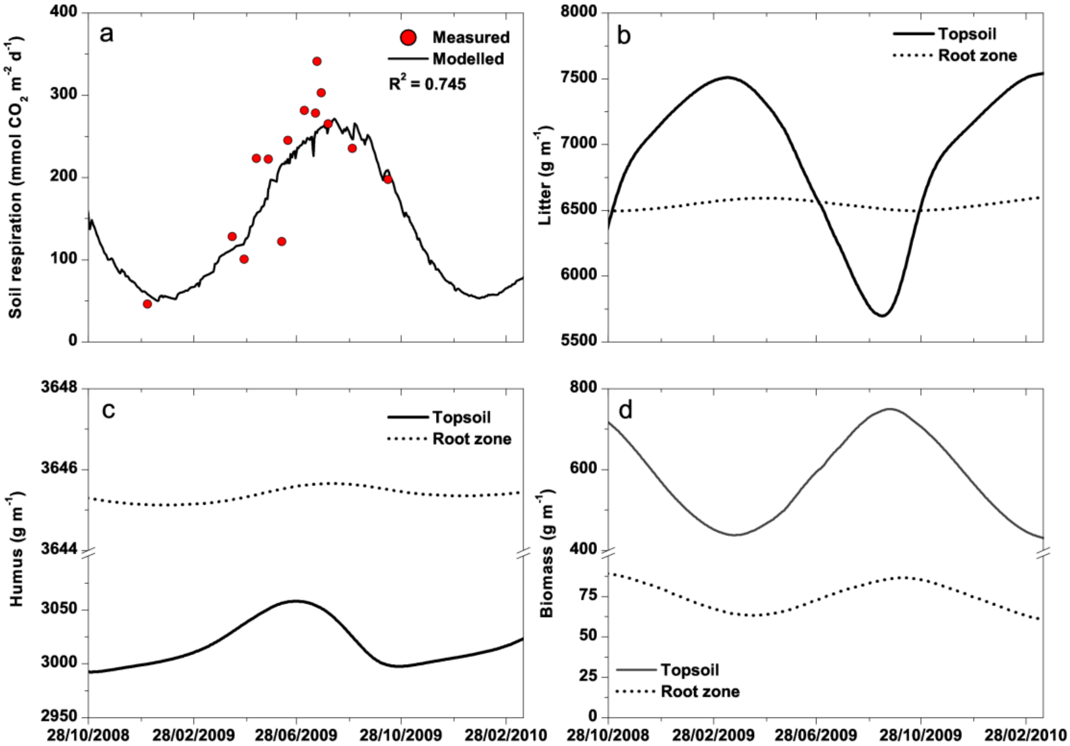
a
Measured
Modelled
R2 = 0.745
Soil respiration (mmol CO2 m-2 d-1)
b
Topsoil
Root zone
Litter (g m-1)
c
Topsoil
Root zone
Humus (g m-1)
d
Topsoil
Root zone
Biomass (g m-1)
28/10/2008
28/02/2009
28/06/2009
28/10/2009
28/02/2010

Fig. 4

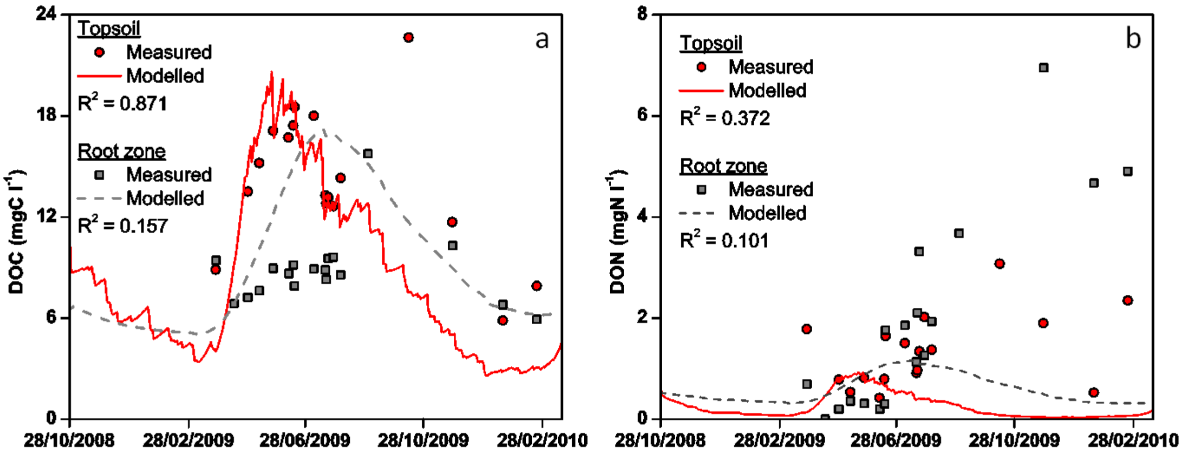

a
Topsoil
Measured
Modelled
R2 = 0.871
Root zone
Measured
Modelled
R2 = 0.157
DOC (mgC l-1)
0
6
12
18
24
28/10/2008
28/02/2009
28/06/2009
28/10/2009
28/02/2010
b
Topsoil
Measured
Modelled
R2 = 0.372
Root zone
Measured
Modelled
R2 = 0.101
DON (mgN l-1)
0
2
4
6
8
28/10/2008
28/02/2009
28/06/2009
28/10/2009
28/02/2010

Fig. 5

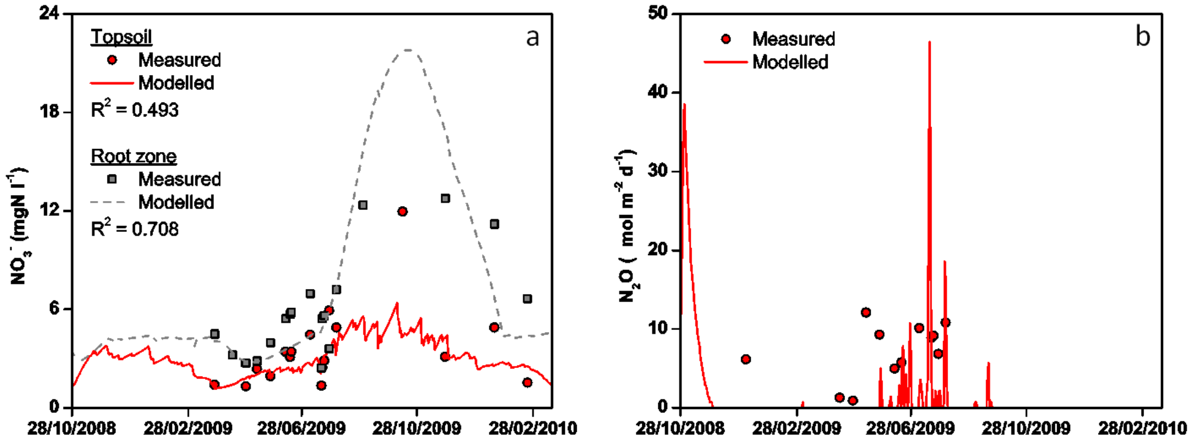
a
Topsoil
Measured
Modelled
R2 = 0.493
Root zone
Measured
Modelled
R2 = 0.708
NO3- (mgN l-1)
0
6
12
18
24
28/10/2008
28/02/2009
28/06/2009
28/10/2009
28/02/2010
b
Measured
Modelled
N2O (mol m-2 d-1)
0
10
20
30
40
50
28/10/2008
28/02/2009
28/06/2009
28/10/2009
28/02/2010

Fig. 6

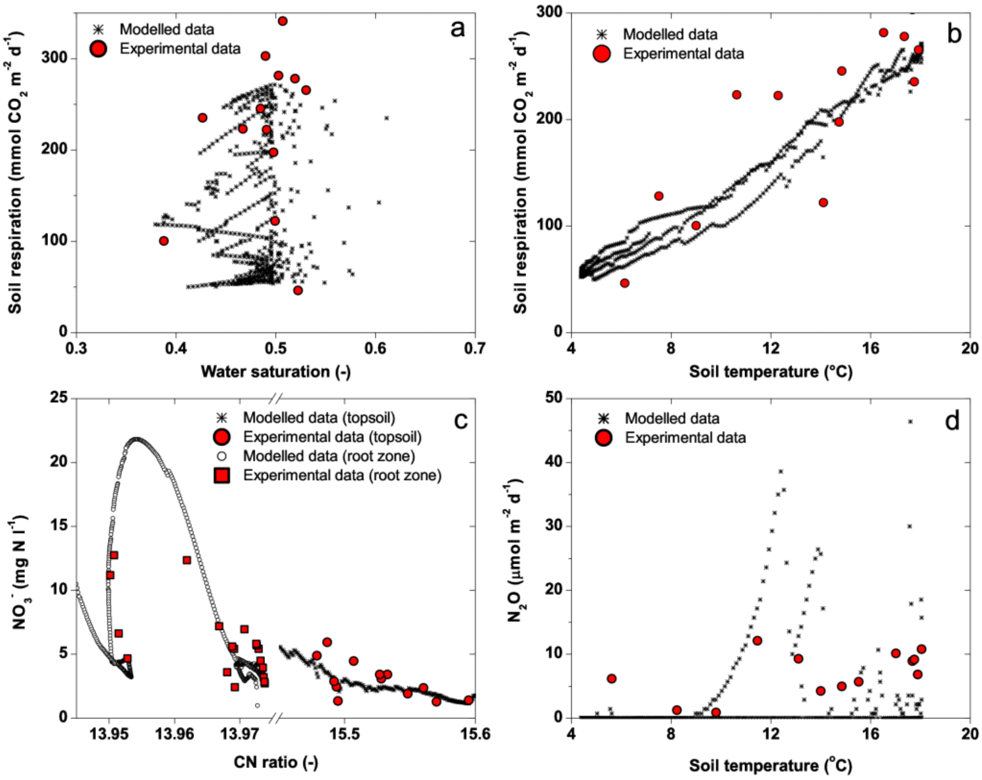

Modelled data
Experimental data
a
Soil respiration (mmol CO2 m-2 d-1)
Water saturation (-)
b
Soil temperature (°C)
c
Modelled data (topsoil)
Experimental data (topsoil)
Modelled data (root zone)
Experimental data (root zone)
NO3- (mg N l-1)
CN ratio (-)
d
N2O (µmol m-2 d-1)

752
753 **Fig. 7**

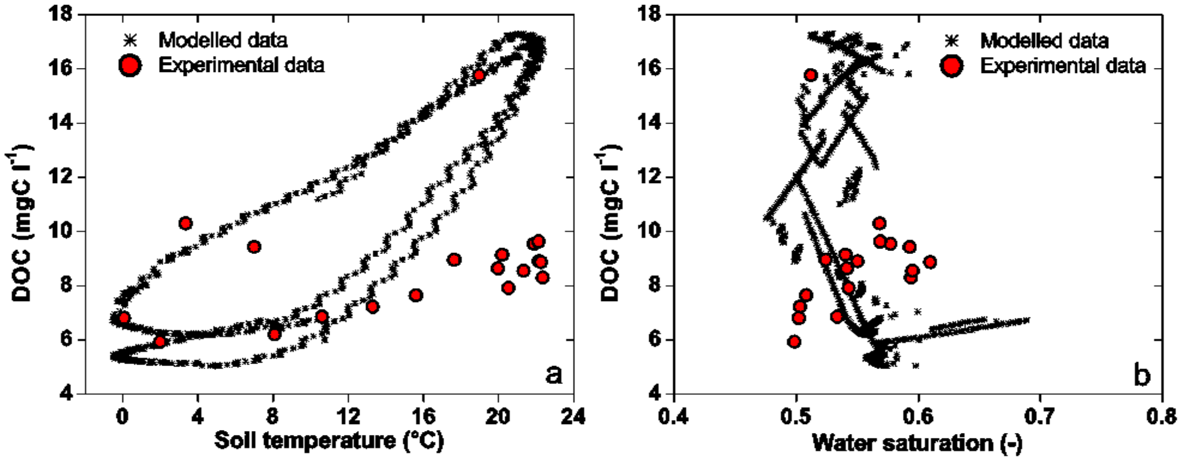
18
16
14
12
10
8
6
4
DOC (mgC l-1)
Modelled data
Experimental data
a
0
4
8
12
16
20
24
Soil temperature (°C)
18
16
14
12
10
8
6
4
DOC (mgC l-1)
Modelled data
Experimental data
b
0.4
0.5
0.6
0.7
0.8
Water saturation (-)

Fig. 8

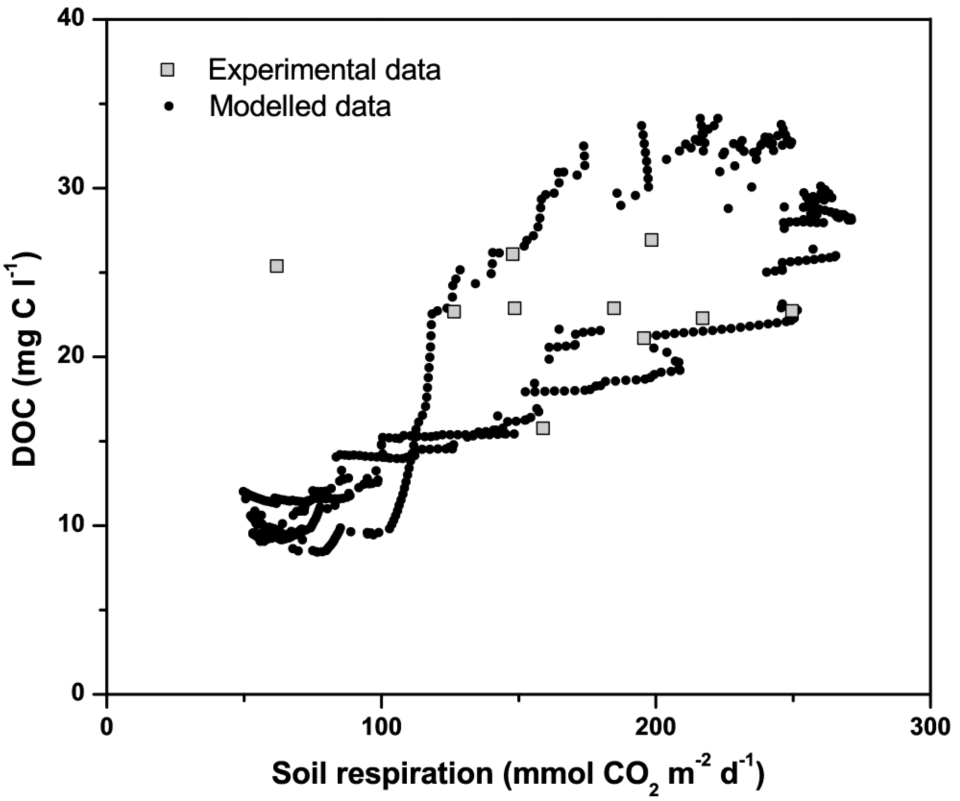

40
30
20
10
0
DOC (mg C l^{-1})
Experimental data
Modelled data
0
100
200
300
Soil respiration (mmol CO_2 m^{-2} d^{-1})

Fig. 9